

# Design of a compact hexagonal structured dual band MIMO antenna using orthogonal polarization for WLAN and satellite applications

Aziz Dkiouak<sup>1</sup>, Mohssine El Ouahabi<sup>2</sup>, Alia Zakriti<sup>3</sup>, Mohsine Khalladi<sup>4</sup>, Aicha Mchbal<sup>5</sup>

<sup>1,2,3</sup>Department of Civil and Industrial Sciences and Technologies, Abdelmalek Essaâdi University, Morocco

<sup>4,5</sup>Faculty of Sciences, Abdelmalek Essaâdi University, Morocco

---

## Article Info

### Article history:

Received Feb 13, 2019

Revised Apr 4, 2019

Accepted Apr 19, 2019

### Keywords:

Envelope correlation coefficient

Diversity gain

MIMO antenna

Mutual coupling

WLAN

X-band satellite

---

## ABSTRACT

In this paper, a compact dual band multiple-input multiple-output (MIMO) antenna system for WLAN and X-band satellite applications (2.4/9.8 GHz respectively) is proposed. On the top face of the substrate, two antenna elements with a size of 20×24 mm<sup>2</sup> are placed side by side and fed with matching orthogonal micro-strip lines. The two antenna elements have orthogonal polarization which can reduce the mutual coupling between its ports. The designed antenna system is fabricated and measured to validate the simulation results. The impedance bandwidths are about 370 MHz (2.19 to 2.56 GHz) and 630 MHz (9.44 to 10.07 GHz), while the obtained isolation is greater than 14 dB at the operating bands. Furthermore, the envelope correlation is less than 0.052 and 0.008 at 2.4 and 9.8 GHz, respectively. Hence the diversity gain is higher than 9.98 in the frequency bands of interest.

Copyright © 2019 Institute of Advanced Engineering and Science.  
All rights reserved.

---

## Corresponding Author:

Aziz Dkiouak,

Department of Civil and Industrial Sciences and Technologies,

National School of Applied Sciences,

Abdelmalek Essaâdi University,

Neighborhood Salam, Av Taha Housin N°4 M'diq, Tetouan, Morocco.

Email: dkiouakaziz@hotmail.fr

---

## 1. INTRODUCTION

According to IEEE standards, the X-band is a range of frequencies in the microwave radio region of the electromagnetic spectrum. This range is allocated by the IEEE at 8.0 and 12.0 GHz. The X-band is widely used in radar applications such as air traffic control, maritime vessel traffic control, vehicle speed detection, people; and natural environment.

Today, MIMO/diversity techniques are largely used in mobile communication, to increase the SNR value, and to improve the channel capacity as well as the data rate in fading environment due to multipath. The utilization of Multiple-Input Multiple-Output (MIMO) system is considered as a key of Wi-Fi, GPS, third generation (3G), fourth generation (4G) and the fifth-generation (5G) wireless communication systems, all in a compact size. This technology has been adopted to achieve high-speed data rate in both reception and transmission, and enhance the quality of service (QOS).

One important requirement for MIMO antenna systems is low mutual coupling between different ports antenna elements. Consequently, since the closely spaced antennas can cause a strong mutual coupling, it is very difficult to achieve a high isolation in a small size, while maintaining good isolation between antenna elements [1]. Several methods for enhancing isolation in MIMO antennas have been reported in the literature. Some effective techniques have been put forward in refs. [2–16], which include: DMN (decoupling and matching network) composed of series/shunt reactive elements [2], eigenmode DMN approach [3],

defected ground structure (DGS) [4-7], electromagnetic band-gap (EBG) [8-11], ELC Resonator [12], neutralization line [13, 14], and using meta-material structure [15, 16].

In this paper, we present a compact hexagonal dual-element MIMO antenna with good isolation at the operating bands. The identical two antenna elements are orthogonally placed in order to achieve orthogonal polarization, which can reduce the mutual coupling between the two antennas and in order to reduce the size of this structure. The proposed MIMO antenna operates at 2.4/9.8 GHz, which covers the WLAN and X-band satellite applications. The MIMO antenna has a small size of  $20 \times 24 \times 1.6 \text{ mm}^3$ , whereas the isolation obtained was higher than 14dB at both frequency bands. The envelope correlation coefficient in the lower and the upper bands is less than 0.052 and 0.008, respectively. On the other hand, a diversity gain of more than 9.98 is obtained at the two interested bands.

## 2. ANTENNA DESIGN

The compact MIMO antenna consists of two hexagonal element antenna systems with an overall size of  $24 \times 20 \text{ mm}^2$ . The two printed hexagonal antenna elements are fed by  $50\Omega$  impedance orthogonal micro-strip feed lines, which are placed symmetrically, and mounted on a 1.6-mm-thick FR4 substrate with a relative permittivity of 4.4 and a loss tangent of 0.02. The structure of the proposed MIMO antenna with detailed dimensions is shown in Figure 1. Different forms on the ground plane are etched to enhance the performance of the proposed MIMO antenna. The detailed dimensions of the proposed MIMO antenna system are illustrated in the Table 1.

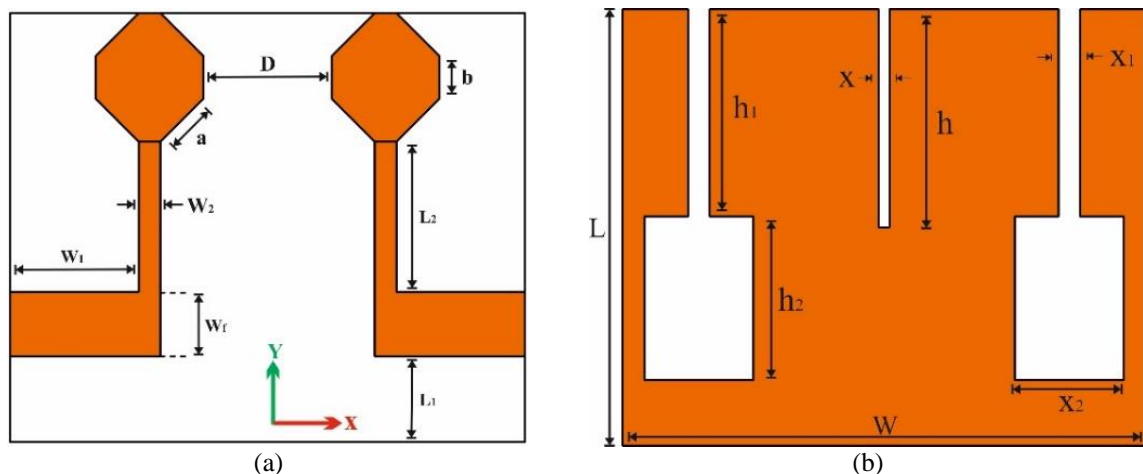


Figure 1. Geometry of the proposed antenna: (a) top view, (b) bottom view

Table 1. Dimensions of the proposed antenna

Parameters	Value (mm)
W	24
L	20
$W_f$	3
$W_1$	5
$W_2$	1
a	2.83
D	6
b	2
$L_2$	7
$L_1$	4
h	10
x	0.5
$h_1$	9.5
$h_2$	7.5
$x_1$	1
$x_2$	5

### 3. ANTENNA ANALYSIS

#### 3.1. S-parameters

In this section, we display the effect of the different slots on the adaptation and the effect of the distance  $D$  between the two monopoles on the isolation, while keeping the other dimensions constant. The simulated results were achieved by using Computer Simulation Technology (CST) Microwave Studio Software. As shown in Figure 2(a), simulation results prove that the two symmetrical hammer-shaped are very important for the appearance of the lower frequency band at 2.4 GHz and simultaneously improve the adaptation at the two bands. Furthermore, when the third slot is etched between two symmetrical hammer-shaped slots, we notice a good enhancement on impedance matching at the lower band.

On the other hand, Figure 2(b) illustrates the simulated  $|S_{21}|$  versus frequency with different values of  $D$ . In this figure, we observe that the isolation increases when the distance grows from 4mm to the desired value 6mm, which means that an acceptable mutual coupling between the two antennas is obtained at the operating bands. Finally, based on the comparison results of the hexagonal antenna, Figure 3 shows the simulated results of the MIMO antenna with optimal dimensions shown in Table 1.

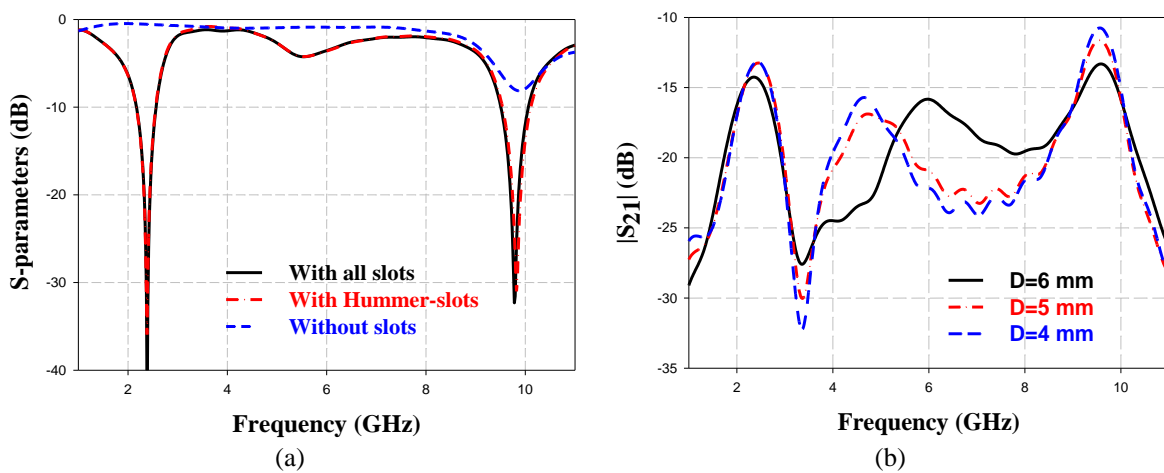


Figure 2. Simulated S-parameters of the proposed antenna: (a)  $|S_{11}|$  and (b)  $|S_{21}|$

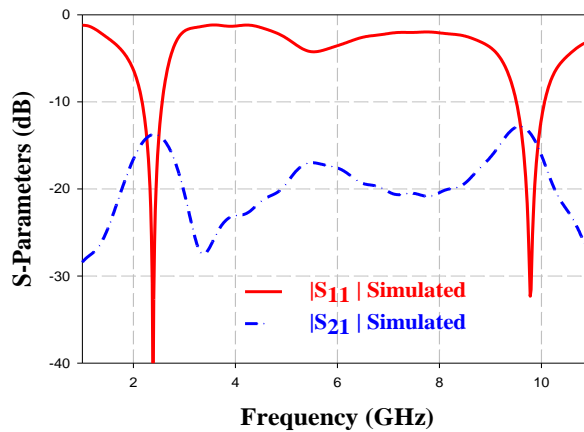


Figure 3. Simulated S parameters of the proposed antenna

According to Figure 3, the reflection coefficient  $|S_{11}|$  is adapted to the desired frequency bands (2.4 GHz - 9.8 GHz), with 45 dB in the lower band and 33 dB in the upper band. The impedance bandwidths are about 450 MHz (2.17 GHz - 2.62 GHz) and 570 MHz (9.50 GHz - 10.07 GHz). The maximum isolation is almost 14 dB at the two operating bands which indicates a good performance of the studied MIMO antenna. Based on the optimal values that illustrated in Table 1, Figure 3 shows the simulated s-parameters of the proposed MIMO antenna.

**3.2. Surface current distributions**

As we can see from Figure 4, the surface current is concentrated around port 1, which means that, a good isolation between antenna elements is maintained. Note that, the effect is the same from port 2 to port 1. Figure 4 depicts the surface current distributions at 2.4 and 9.8 GHz when two ports are excited simultaneously.

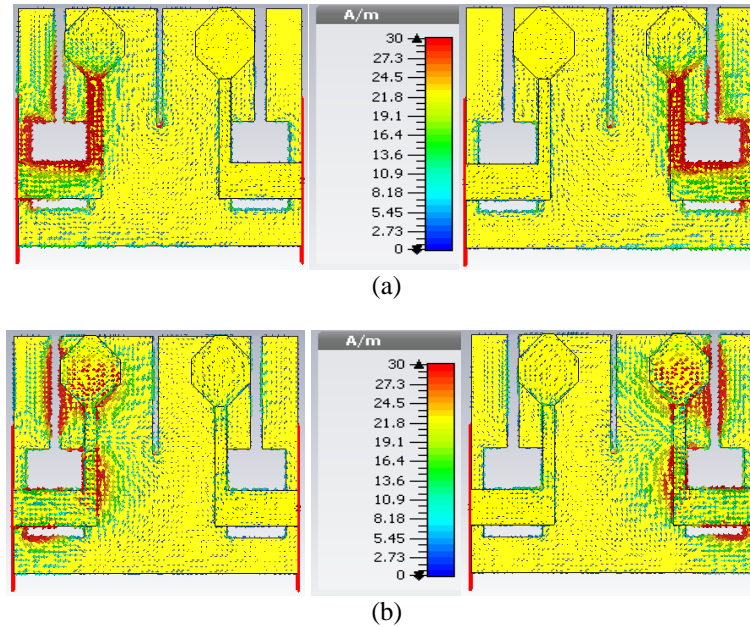


Figure 4. The surface current distributions of the two ports at: (a) 2.4 GHz and (b) 9.8 GHz

**3.3. Envelope correlation coefficient and diversity gain**

The envelope correlation coefficient (or correlation between the envelopes of the signals) [17] is used to measure the correlation between the two-antenna elements. This correlation coefficient should be a small value, in order to indicate a high diversity between the two MIMO antenna elements. The ECC between the  $i^{th}$  and  $j^{th}$  antenna elements using far-field patterns can be expressed as:

$$ECC(i, j) = \frac{\left( \oint (X_{PR} E_{\theta i}(\Omega) E_{\theta j}^*(\Omega) P_{\theta}(\Omega) + E_{\phi i}(\Omega) E_{\phi j}^*(\Omega) P_{\phi}(\Omega)) d(\Omega) \right)^2}{\oint (X_{PR} G_{\theta i}(\Omega) P_{\theta}(\Omega) + G_{\phi i}(\Omega) P_{\phi}(\Omega)) d(\Omega) \oint (X_{PR} G_{\theta j}(\Omega) P_{\theta}(\Omega) + G_{\phi j}(\Omega) P_{\phi}(\Omega)) d(\Omega)} \quad (1)$$

Where,  $X_{PR}$  denotes cross-polarization power ratio of the propagation environment.  $G_{\theta}(\Omega)$  and  $G_{\phi}(\Omega)$  are the power patterns of  $\theta$  and  $\phi$  polarizations, respectively.  $P_{\theta}(\Omega)$  and  $P_{\phi}(\Omega)$  denote the angular density functions of the  $\theta$  and  $\phi$  polarizations, respectively.

$E_{\theta i}(\Omega)$  and  $E_{\theta j}(\Omega)$  are the electric field patterns of the  $i^{th}$  and  $j^{th}$  antenna elements in the  $\theta$  polarization, respectively.  $E_{\phi i}(\Omega)$  and  $E_{\phi j}(\Omega)$  are the electric field patterns of the  $i^{th}$  and  $j^{th}$  antenna elements in the  $\phi$  polarization, respectively. In the case of uniform multipath environment,  $X_{PR} = 1$  and  $P_{\theta}(\Omega) = P_{\phi}(\Omega) = \frac{1}{4\pi}$ . The envelope correlation coefficient ECC for two antennas can be approximated as follow:

$$ECC = \frac{\left( \oint (E_{\theta 1}(\Omega) E_{\theta 2}^*(\Omega) + E_{\phi 1}(\Omega) E_{\phi 2}^*(\Omega)) d(\Omega) \right)^2}{\oint (G_{\theta 1}(\Omega) + G_{\phi 1}(\Omega)) d(\Omega) \oint (G_{\theta 2}(\Omega) + G_{\phi 2}(\Omega)) d(\Omega)} \quad (2)$$

Where,  $E_1$  and  $E_2$  are the far-field radiation patterns, generated from ports 1 and 2 respectively.

Figure 5 represents the simulated envelope correlation coefficient of the proposed MIMO antenna from far-field patterns. As observed from this figure, the ECC is very low at the operated frequency bands, which are about 0.052 at 2.4 GHz and 0.008 at 9.8 GHz. As can see from the Figure 5, the severe coupling between the antenna elements at the lower band causes an envelope correlation of around 0.052, which is much lower than the rule of thumb threshold of 0.5, the same thing for the correlation of the upper band which is negligibly small.

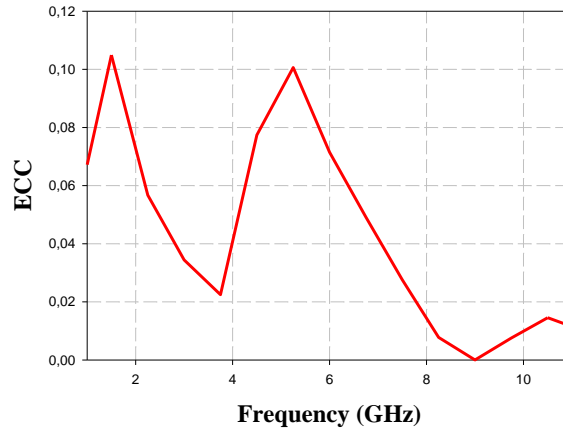


Figure 5. The envelope correlation curve

The diversity gain is then obtained as a ratio of the SNR of the combined signal relative to that of a reference signal at a given probability level. The relation between diversity gain and correlation coefficient can be given by the following approximate expression [18].

$$DG = 10\sqrt{1 - |\rho|^2} \quad (3)$$

Where  $\rho$  is the complex cross correlation coefficient, and  $|\rho|^2 \approx ECC$ . As shown in Figure 6, the value of the presented MIMO antenna diversity gain is around 10 dB across the both operating frequency bands. Figure 6 illustrates the DG of the designed MIMO antenna.

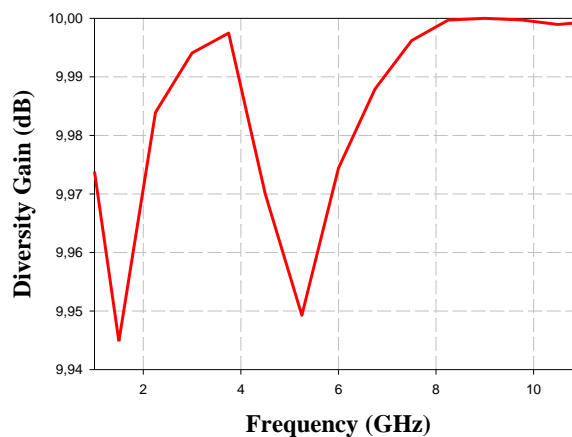


Figure 6. Diversity gain of the proposed MIMO

## 4. FABRICATION AND MEASURED RESULTS

### 4.1. S-parameters

In order to validate the simulated results, we have fabricated and tested the proposed MIMO antenna. The fabrication process is carried out at AbdelMaleK Essaâdi University Laboratories. It is done

using a printed circuit board (PCB) milling machine: The LPKF Protomat E33. Figure 7 shows a photograph of the fabricated antenna. The simulated and measured S-parameters of the proposed MIMO antenna are compared in Figure 8 and listed in Table 2. The measured results were obtained by using a Rohde and Schwarz ZVB 20 vector network analyzer.

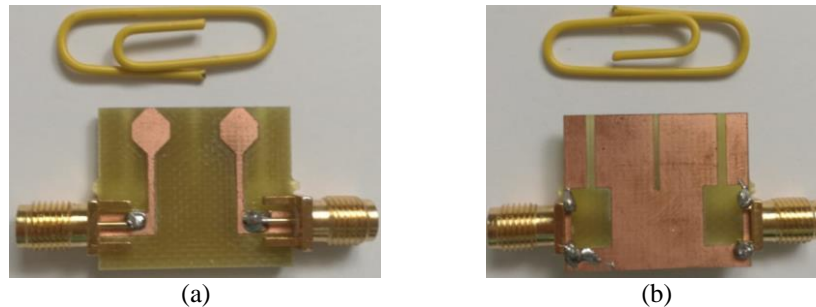


Figure 7. Photograph of the fabricated antenna: (a) front view, (b) back view

It is observed that the return and insertion loss curves of an overall trend between simulated and measured results are almost well matched except that the measured  $|S_{11}|$  shifts a little higher than the simulated one. This is due to the fabricated imperfections, the loss of the feeding cable used in measurement, and connectors. Since the two antenna elements are symmetrically placed, only  $|S_{11}|$  and  $|S_{21}|$  are represented. The measured results for  $|S_{11}| < 10$  of the two frequency bands are about 460 MHz (2.31-2.77 GHz) resonated at 2.4 GHz, and 530 MHz (9.63-10.20 GHz) resonated at 9.8GHz, which correspond to WLAN and satellite applications. Meanwhile, the measured isolation is better than 27 dB and 17 dB in both lower and upper bands respectively, which indicates the proposed MIMO antenna good performance.

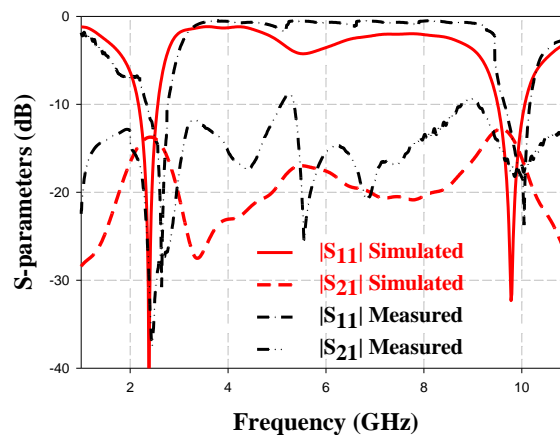


Figure 8. Simulated and measured S-parameters of the proposed MIMO antenna

Table 2. Measured and simulated impedance bandwidths of the proposed dual-band MIMO antenna

	Lower band		Upper band	
	$F_L$ (GHz)	BW (GHz)	$F_U$ (GHz)	BW (GHz)
Measured	2.46	2.31 - 2.77	10.03	9.63_10.20
Simulated	2.4	2.17 - 2.62	9.8	9.50 - 10.07

#### 4.2. Radiation patterns

The measured and the simulated radiation patterns of the proposed MIMO antenna at the frequencies of 2.4 GHz and 9.8 GHz in the E-Plane and H-Plane when port one is excited and other port terminated with a 50- $\Omega$  load are presented in Figures 9. As shown in Figure 9, there is a good agreement

between the simulated and measured gain patterns at both frequency bands. However, the slight difference between the measured and simulated radiation patterns comes principally from the measurement setup such as angle calibration which causes the deviation between measured and simulated phi in x-y plane, and the measurement is not carried out in an anechoic chamber. Figure 9 shows the simulated and measured radiation patterns of the presented MIMO antenna at 2.4 and 9.8 GHz.

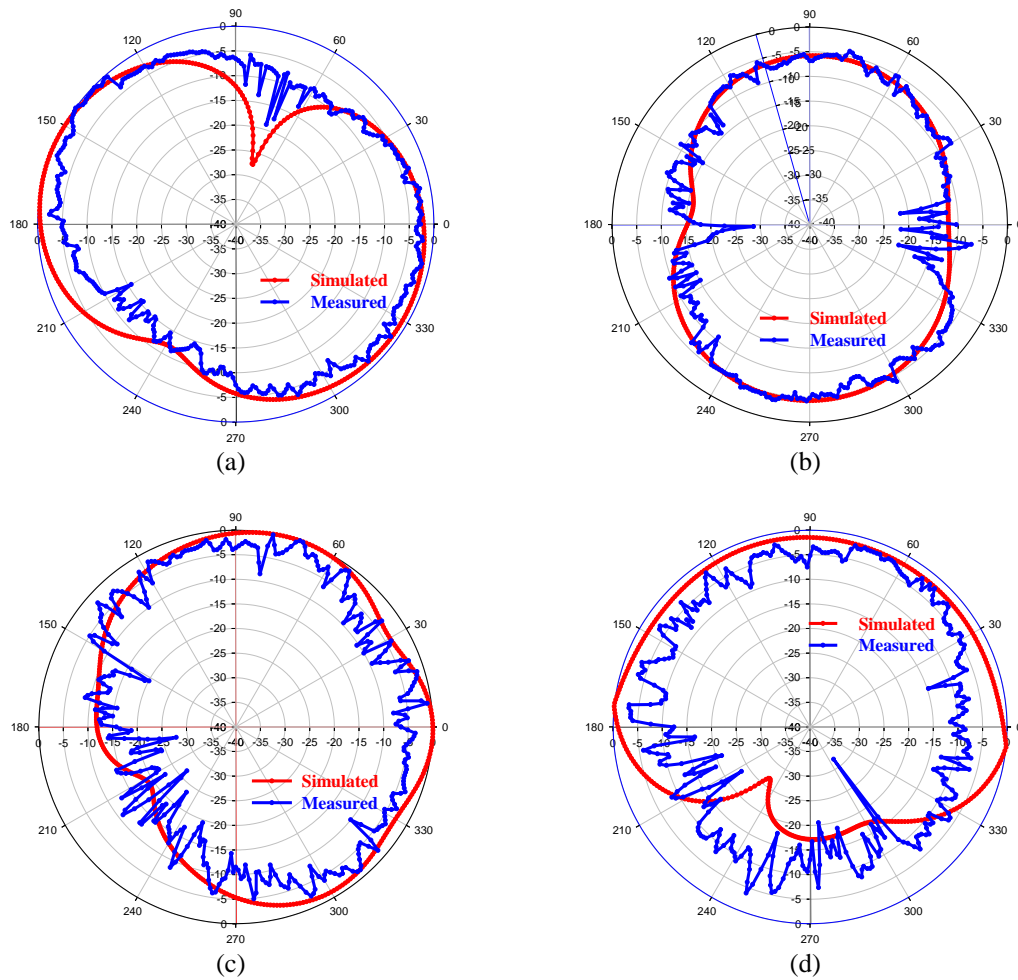


Figure 9. Simulated and measured radiation patterns of the MIMO antenna at frequencies: (a) E-plane at 2.4 GHz, (b) H-plane at 2.4 GHz, (c) E-plane at 9.8 GHz, (d) H-plane at 9.8 GHz

**5. PERFORMANCE COMPARAISON**

In this section, we compare some parameters of the proposed MIMO antenna by some other reported MIMO antenna. The comparison has been done in terms of the bandwidth, envelope correlation coefficient, size and isolation. Table 3 represents the Performance comparisons between the proposed MIMO antenna and other reported antennas. After the comparison, we can say that the presented antenna with a compact size and an acceptable isolation is suitable for MIMO system applications.

Table 3. Performance comparisons of the proposed and reported MIMO antennas

Ref.	Size (mm <sup>3</sup> )	Bandwidth (GHz)	Isolation (dB)	Permittivity $\epsilon_r$	ECC	Sub.
Article	24 × 20 × 1.6	2.35 - 3.05 & 5.12 - 5.51	15	4.4	0.052	FR4
[2]	36×30.16×1.5	2.3-2.78 & 3.31 to 3.9	20	4.3	0.0012	FR4
[3]	34 × 36 × 1.5	2.136 to 2.55 & 3.3 to 3.859	16.8	4.3	0.0034	FR4
[19]	43 × 38 × 1.6	2.35–3.05 & 5.12–5.51	12	4.4	0.001	FR4
[20]	1.6 × 52 × 77.5	2.40-2.48 & 5.15-5.82	15	4.4	0.2	FR4

## 6. CONCLUSION

In this article, a compact dual band MIMO antenna for WLAN and X-band satellite applications is presented. The prototype antenna is fabricated and measured. From the measurement results, we show that a low mutual coupling of less than 27 dB at 2.4 GHz and 17 dB at 9.8 GHz was achieved. The envelope correlation coefficient is less than 0.052 and a diversity gain more than 9.98 dB were obtained, which is promising for good antenna diversity. In addition the MIMO antenna is characterized by a simple structure, low cost FR-4 substrate and a compact size of 24×20 mm<sup>2</sup>; compared with the reported antennas. Thus, the proposed MIMO antenna is very adequate for WLAN and X-band satellite applications.

## ACKNOWLEDGEMENTS

The authors would like to thank Professor Naima Amar Touhami of Abdelmalek Essaâdi University, for his patient discussion on this paper.

## REFERENCES

- [1] A. Ozdemir M. and E. Arvas, "Dynamics of spatial correlation and implications on MIMO systems," *IEEE Communications Magazine*, vol. 42, no. 6, Jun 2004.
- [2] Weber J., C. Volmer K. Blau, R. Stephan and M. A. Hein, "Miniaturized antenna arrays using decoupling networks with realistic elements," *IEEE Trans. Microw. Theory Tech.*, vol. 54, no. 6, pp. 2733-2740, Jun 2006.
- [3] S.-L. Zuo, Y.-Z. Yin, Z.-Y. Zhang, W.-J. Wu, J.-J. Xie, "Eigenmode decoupling for MIMO loop-antenna based on 180° coupler," *Progress In Electromagnetics Research Letters*, 2011.
- [4] L. H. Weng, Y. C. Guo, X. W. Shi and X. Q. Chen, "An overview on defected ground Structure," *Progress In Electromagnetics Research B*, 2008.
- [5] Y. Yu, M. Yuan and L. Wu, "A Compact Printed Monopole Array With Defected Ground Structure To Reduce The Mutual Coupling," *J. Electromagn. Waves Appl.*, 2011.
- [6] A. S. Bhadouria and M. Kumar, "Microstrip X-band Antenna with improvement in Performance Using DGS," *Electrical and Electronic Engineering*, 2014.
- [7] S. Kamal and A. Chaudhari, "Printed Meander Line MIMO Antenna Integrated with Air Gap, DGS and RIS: A Low Mutual Coupling Design for LTE Applications," *Progress In Electromagnetics Research C*, 2017.
- [8] N. Jaglan, S. D. Gupta, B. K. Kanaujia, S. Srivastava and E. Thakur, "Triple Band Notched DG-CEBG Structure Based UWB MIMO/Diversity Antenna," *Progress In Electromagnetics Research C*, 2018.
- [9] N. Kumar and U. K. Kommuri, "MIMO Antenna Mutual Coupling Reduction for WLAN Using Spiro Meander Line UC-EBG," *Progress In Electromagnetics Research C*, 2018.
- [10] Dabas T., Gangwar D., Kanaujia B. K. and Gautam A. K., "Mutual coupling reduction between elements of UWB MIMO antenna using small size uniplanar EBG exhibiting multiple stop bands," *AEU - International Journal of Electronics and Communications*, 2018.
- [11] X. Zhang, X. Zhong, B. Li, and Y. Yu, "A Dual-Polarized MIMO Antenna with EBG for 5.8 GHz WLAN Application," *Progress In Electromagnetics Research Letters*, vol. 51, pp. 15–20, 2015.
- [12] S. Pandit, A. Mohan, P. Ray, "A Compact Planar MIMO Monopole Antenna with Reduced Mutual Coupling for WLAN Applications using ELC Resonator," *Proceedings of the Asia-Pacific Microwave Conference*, 2016.
- [13] Y. Wang and Z. Du, "A Wideband Printed Dual-Antenna System with a Novel Neutralization Line for Mobile Terminals," *IEEE Antennas and Wireless Propagation Letters*, 2013.
- [14] Zhang S. and Pedersen G. F., "Mutual Coupling Reduction for UWB MIMO Antennas With a Wideband Neutralization Line," *IEEE Antennas and Wireless Propagation Letters*, vol. 15, pp. 166-169, 2016.
- [15] Y. Lee, H. Chung, J. Ha and L. Choi, "Design of a MIMO antenna with improved isolation using meta-material," *International Workshop on Antenna Technology (iWAT'11)*, 2011.
- [16] Y. Torabi, A. Bahri and A. -R. Sharifi, "A Novel Metamaterial MIMO Antenna with Improved Isolation and Compact Size Based on LSRR Resonator," *IETE Journal Of Research*, 2015.
- [17] J. Zhang, J. OuYang, K. Z. Zhang and F. Yang, "A Novel Dual-Band MIMO Antenna with Lower Correlation Coefficient," *International Journal of Antennas and Propagation*, 2012.
- [18] E. R. Iglesias, "Printed Multi-Band MIMO Antenna Systems and Their Performance Metrics," *IEEE Antennas and Propagation Magazine*, 2013.
- [19] A. Dkiouak, A. Zakriti, M. El Ouahabi, A. Zugari and M. Khalladi, "Design of a Compact MIMO Antenna for Wireless Applications," *Progress In Electromagnetics Research M*, 2018.
- [20] A Deng J., Li J., Zhao L. and Guo L., "A Dual-Band Inverted-F MIMO Antenna With Enhanced Isolation for WLAN Applications," *IEEE Antennas and Wireless Propagation Letters*, 2016.

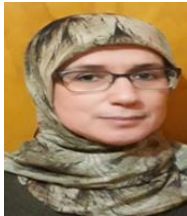


**BIOGRAPHIES OF AUTHORS**

**Aziz Dkiouak** was born in December 1985, in Tayjoute town, 30 Km from Chefchaouen, Morocco. He received the Master's degree in Electronics and Telecommunications at the Faculty of Sciences, Abdelmalek Essaâdi University, Tetuan, Morocco in 2010. He is currently working on a Ph.D. degree and His research focuses on the design and realization of MIMO antennas with low mutual coupling for wireless applications.



**Mohssine El Ouahabi** was born in 1987 M'diq, Morocco. He received a Master degree in Telecommunication systems engineering from Abdelmalek Essaâdi University, Tetuan, Morocco, in 2013. He is currently working toward on a PhD degree in microwave circuits using the metamaterial structure at the same University.



**Alia Zakriti** received PhD degree in Electrical Engineering in 2001 from University Abdelmalek Essaâdi (UAE), Morocco. During 2004-2010, she was professor at Caddi Ayad University, Morocco. Since 2010, she joined the National School of Applied Sciences, UAE, as a Professor of Electrical Engineering. She directed a Research Unit "Advanced Science and Technology" during several years and she was also a head of department of Civil and Industrial Sciences and Technologies. Her research interests focus mainly on printed microwave circuits and embedded systems. She has authored and co-authored several papers in international refereed journals and conferences in the field of microwave communications Technology.



**Mohsine Khalladi** was born in Tangier, Morocco. He received the "Licence en physique" in 1988 from the University of Abdelmalek Essaâdi, Tetuan, Morocco and Ph. D. degree in physics from the University of Granada, Spain, in 1994. In September 1996, he joined the Faculty of Sciences of Abdelmalek Essaâdi University as an associate professor and was promoted to the rank of full Professor in September 2000. He is currently the head of Electronics and Microwaves Group 'EMG' and the responsible of the Telecommunication and Information systems laboratory 'LaSIT'. His main fields of interest concern mainly the time-domain numerical solution of scattering and radiation electromagnetic problems.



**Aicha Mchbal** is a phd student, her doctoral research investigates the enhancement of mimo antenna performances, she holds a master's degree in telecommunication systems engineering from the abdelmalek Essaâdi university of tetuan, morocco. she authored the article " mutual coupling reduction using a protruded ground branch structure in a compact UWB owl-shaped mimo antenna